

# CONTROL OF BIFURCATION OF DC/DC BUCK CONVERTERS CONTROLLED BY DOUBLE - EDGED PWM WAVEFORM

**A. Elbkosh, D. Giaouris, B. Zahawi & V. Pickert**

*School of Electrical, Electronic and Computer Engineering,  
Newcastle University, UK*

[Damian.Giaouris@ncl.ac.uk](mailto:Damian.Giaouris@ncl.ac.uk)

**S. Banerjee**

*Centre for Theoretical Studies and Department of Electrical Engineering,  
Indian Institute of Technology, Kharagpur, India*

[soumitro@ee.iitkgp.ernet.in](mailto:soumitro@ee.iitkgp.ernet.in)

## Abstract

The nonlinear behaviour of the buck converter controlled by double-edged PWM waveform is studied in this paper. The stability of the system is analyzed using the state transition matrix over one switching cycle (the monodromy matrix) including the state transition matrices during each switching (saltation matrices). Three supervising control methods are applied to extend the normal period one operation of the system. Good agreement is demonstrated between theoretical analysis, numerical simulations and the results are experimentally verified.

## Key words

DC/DC converters, PWM, monodromy matrix, control of bifurcations.

## 1 Introduction

Pulse width modulation (PWM) is the most frequently used control method for switching converters. Conventionally a saw-tooth signal is compared with a control signal to produce a series of pulses that control the states of the power electronic switches. The nonlinear effects of these switchings have been extensively studied in the past and various methods have been proposed for their analysis and control [Verghese, Elbuluk and Kassakian, 1986], [Chakrabarty, Poddar and Banerjee, 1996], [Di Bernardo, Garofalo, Glielmo and Vasca, 1998], and [Tse, 2003]. Most of these methods assume that the saw-tooth signal is discontinuous at  $t=T$ , where  $T$  is the period of the signal. This, however, is not a valid approximation at high frequencies where the signal looks more like an asymmetric triangular wave. Such a system demands a fresh look at its bifurcations and chaotic behaviour.

The control of a chaotic response has been the focus of extensive research such as the Ott-Grebogi-Yorke (OGY) method [Ott, Grebogi and Yorke, 1990] and linear Time Delayed Feedback Control (TDFC) method [Bleich, and Socolar, 1996] and [Pyragas, 2001] which are designed to stabilize one of the unstable periodic orbits that exist in a chaotic system. However, these controllers may require high processing power and are not always applicable to real systems with small signal to noise ratio. An alternative method has been proposed by the authors which is simpler, easier to implement, and greatly extends the stable operating region of the converter [Giaouris, Banerjee,

Zahawi and Pickert, 2008] and [Giaouris, Elbkosh, Pickert, Zahawi and Banerjee, 2006]. This method is based on changing the state transition matrices during the switchings in such a way that the eigenvalues of the system remain within the unit circle. In this paper, the analysis is extended by applying this method to DC/DC buck converters controlled by double-edged PWM waveform.

The paper is organized as follows: Section two briefly outlines the operation of the DC/DC buck converter and its dynamic equations. Section three shows the bifurcation behaviour of the system. In Section four, we analyse the stability of the system based on the complete cycle solution matrix of the system (the monodromy matrix). Finally, we apply three control methods based on the proposed analysis to maintain the stability of the system over a much wider range of input parameters. Analytical, numerical and experimental results validate the proposed controllers.

## 2 System Descriptions and Operation

Fig. 1(a) shows a simplified block diagram that describes the voltage mode controlled buck converter.

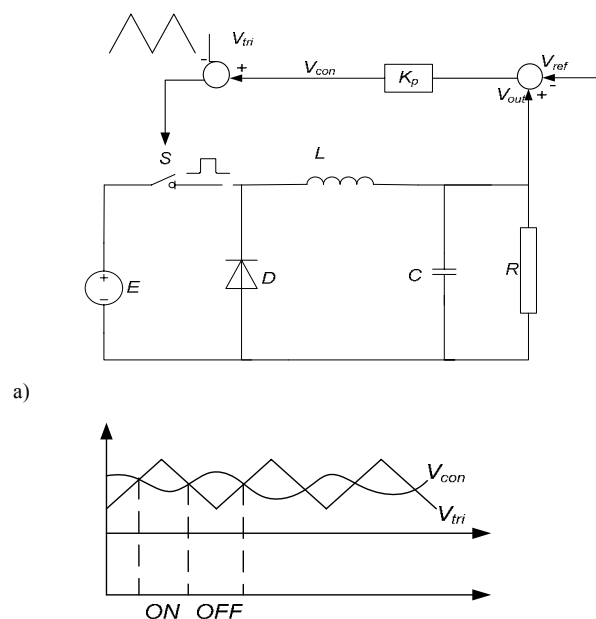


Figure 1. (a) Block diagram of the buck converter with voltage controller, (b) the generation of switching signal.

The switch  $S$  is controlled by a comparator which compares the control signal  $V_{con}$  with a suitable periodic triangular waveform  $V_{tri}$  and a switching occurs when these two signals become equal (Fig. 1b). The triangular signal can be written as:

$$V_{tri} = \begin{cases} \frac{2\Delta V}{T}t + V_U & 0 < t < 0.5T \\ -\frac{2\Delta V}{T}t + \Delta V + V_U & 0.5T \leq t < T \end{cases} \quad (1)$$

where  $V_U, V_L$  are the upper and lower limit of the triangular signal and  $\Delta V = V_U - V_L$ . The state equations that represent the states during a switching cycle are:

$$\dot{\mathbf{x}} = \begin{cases} \mathbf{A}_s \mathbf{x} + \mathbf{B}_1 E, & S = Off \\ \mathbf{A}_s \mathbf{x} + \mathbf{B}_2 E, & S = On \end{cases} \quad (2)$$

where  $\mathbf{x} = [v_{out} \ i_L]^T = [x_1 \ x_2]^T$ ,  $E$  is the input voltage and  $\mathbf{A}_s, \mathbf{B}$  are the system matrices given by:

$$\mathbf{A}_s = \begin{bmatrix} -1/RC & 1/C \\ -1/L & 0 \end{bmatrix}, \mathbf{B}_1 = \begin{bmatrix} 0 \\ 0 \end{bmatrix} \text{ and } \mathbf{B}_2 = \begin{bmatrix} 0 \\ 1/L \end{bmatrix}$$

### 3 Bifurcation Behaviour

In general, the circuit gives an average dc output voltage close to the desirable value with a periodic ripple equal to the period of the driving clock (the triangular signal) as shown in Fig. 2. However, by increasing the input voltage a smooth period doubling bifurcation renders the system unstable and almost instantly a nonsmooth bifurcation forces the system into a chaotic region (Figs. 3 & 4).

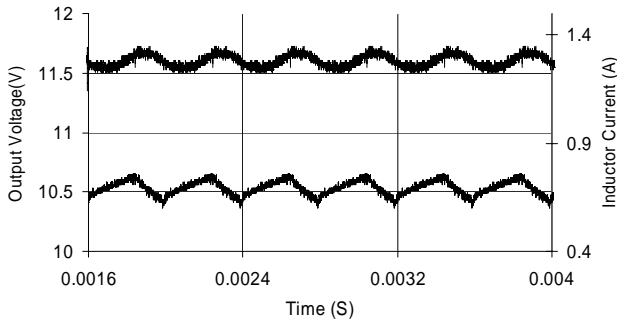


Figure 2. Experimental result, Period-1 operation at input voltage of 20 volt,  $V_{ref} = 11.3$  V,  $K_p = 8.4$ ,  $L = 0.002$  H,  $C = 47\mu\text{F}$ ,  $R = 22\ \Omega$ ,  $T = 400\ \mu\text{s}$ ,  $V_L = 3.8$  V,  $V_U = 8.2$  V

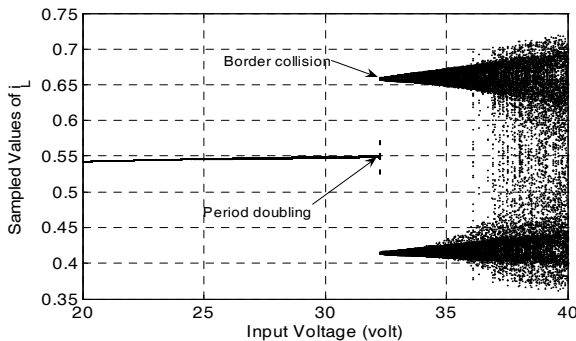


Figure 3. Bifurcation diagram with input voltage as bifurcation parameter

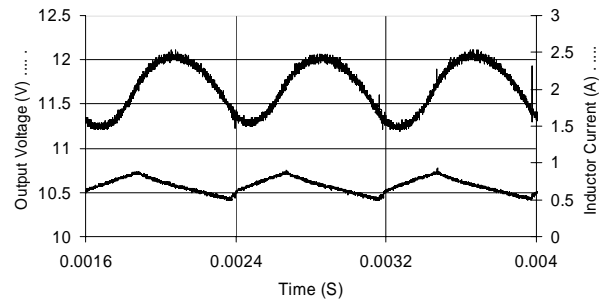


Figure 4. The period-2 response of the system at input voltage of 34 V

This non-smooth bifurcation occurs when the periodic solution of the system touches the non-smooth hypersurface (i.e., the upper or lower part of the triangular signal) [Banerjee, Ott, Yorke and Yuan, 1997], [Yuan, Banerjee, Ott and Yorke, 1998], [Banerjee and Verghese, 2001] and [Tse and Di Bernardo, 2002].

### 4 Stability Analysis of the System

The stability analysis of a saw-tooth controlled DC/DC converter is usually based on the derivation of the Poincaré map of the system [Verghese, Elbuluk and Kassakian, 1986], [Banerjee and Chakrabarty, 1998], [Di Bernardo and Vasca, 2000] and [Fang and Abed, 2001]. Other methods include trajectory sensitivity [Hiskens and Pai, 2000] and auxiliary vectors [Dranga, Buti, Nagy and Funato, 2005]. A different approach, based on the system saltation matrices [Aizerman and Gantmakher, 1958], [Filippov, 1988], [Baushev, Zhusubaliyev, Kolokolov, and Terekhin, 1992] and [Zhusubaliyev, Soukhoterlin, and Mosekilde, 2001] as previously applied to non-smooth mechanical systems [Leine, Campen and Vrande, 2000] and [Leine and Nijmeijer, 2004], has been proposed by the authors and applied to DC/DC converters with fruitful results [Giaouris, Banerjee, Zahawi and Pickert, 2008], [Giaouris, Elbkosh, Pickert, Zahawi and Banerjee, 2006] and [Giaouris, Elbkosh, Banerjee, Zahawi and Pickert, 2006]. One of the advantages of this method is that it treats each switching separately and hence the overall analysis is simpler than the conventional Poincaré map approach. Furthermore, the analysis it offers an insight into the operation of the system and its loss of stability, and hence makes it possible to derive new control laws to extend the stable operating region [Giaouris, Banerjee, Zahawi and Pickert, 2008].

The application of the scheme to converters that use a triangular carrier wave imposes new challenges as the trajectory crosses two switching manifolds at  $t = d_1T$  and  $t = d_2T$  (Fig. 5).

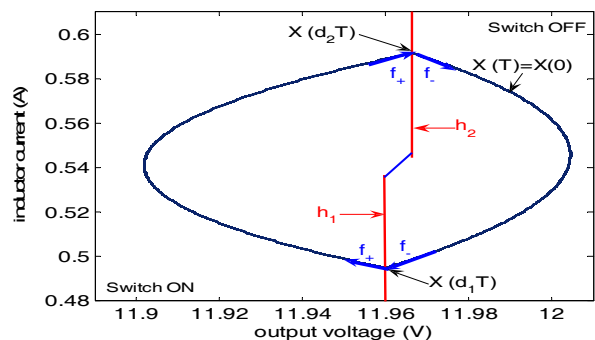


Figure 5. Period-1 orbit of the system

The monodromy matrix of the system consists of the fundamental solution matrices during the smooth areas and the saltation matrices during the switchings [Leine and Nijmeijer, 2004]:

$$\mathbf{M}(T, X_0, 0) = e^{\mathbf{A}_s(d_2-d_1)T} \times \mathbf{S}_2 \times e^{\mathbf{A}_s(d_2-d_1)T} \times \mathbf{S}_1 \times e^{\mathbf{A}_s d_1 T} \quad (3)$$

where  $\mathbf{S}_2$  and  $\mathbf{S}_1$  are the saltation matrices at the switching time  $d_2T$  and  $d_1T$ , respectively [Leine and Nijmeijer, 2004], and can be calculated from:

$$\mathbf{S} = \mathbf{I} + \frac{(\mathbf{f}_+(x(t_\Sigma), t_\Sigma) - \mathbf{f}_-(x(t_\Sigma), t_\Sigma)) \mathbf{n}^T}{\mathbf{n}^T \mathbf{f}_-(x(t_\Sigma), t_\Sigma) + \frac{\partial h}{\partial t}(x(t_\Sigma), t_\Sigma)} \quad (4)$$

where  $h$  is the switching manifold,  $\mathbf{n}$  is the normal to  $h$ ,  $\mathbf{I}$  is the identity matrix,  $t_\Sigma$  is the switching time,  $\mathbf{f}_-$  and  $\mathbf{f}_+$  are the two smooth vector fields before and after the switching. From the circuit topology, it can be deduced that the two switching manifolds are:

$$\begin{aligned} h_1(\mathbf{x}, t) &= Kp(x_1(t) - V_{ref}) - (V_U + 2\Delta V d_1) \\ h_2(\mathbf{x}, t) &= Kp(x_1(t) - V_{ref}) - (\Delta V + V_U) - 2\Delta V d_2 \end{aligned} \quad (5)$$

The perpendicular vectors onto these surfaces are:

$$\begin{aligned} \mathbf{n}_1 &= \begin{bmatrix} \frac{\partial h_1}{\partial x_1} & \frac{\partial h_1}{\partial x_2} \end{bmatrix}^T = [k_p \quad 0]^T \\ \mathbf{n}_2 &= \begin{bmatrix} \frac{\partial h_2}{\partial x_1} & \frac{\partial h_2}{\partial x_2} \end{bmatrix}^T = [k_p \quad 0]^T \end{aligned}$$

At the time instant  $t = d_1T$  the switching condition  $h_1(\mathbf{x}, d_1T) = 0$  is satisfied and hence a switching takes place from  $\mathbf{f}_-(x(d_1T)) = \mathbf{A}_s \mathbf{x} + \mathbf{B}_1 E$  to  $\mathbf{f}_+(x(d_1T)) = \mathbf{A}_s \mathbf{x} + \mathbf{B}_2 E$ . The saltation matrix at this point is calculated from (4):

$$\mathbf{S}_1 = \mathbf{I} + \begin{bmatrix} 0 & 0 \\ \frac{E/L}{(x_2(d_1T) - x_1(d_1T)/R) - (V_U - V_L)} & 0 \\ \frac{0}{C} & \frac{0}{0.5T \times K_p} \end{bmatrix} \quad (6)$$

At  $t = d_2T$ , there is another switching as  $h_2(\mathbf{x}, d_2T) = 0$ . The two vector fields before and after the switching are  $\mathbf{f}_+(x(d_2T)) = \mathbf{A}_s \mathbf{x} + \mathbf{B}_2 E$  &  $\mathbf{f}_-(x(d_2T)) = \mathbf{A}_s \mathbf{x} + \mathbf{B}_1 E$ . The state transition matrix at this point is

$$\mathbf{S}_2 = \mathbf{I} + \begin{bmatrix} 0 & 0 \\ \frac{-E/L}{(x_2(d_2T) - x_1(d_2T)/R) + (V_U - V_L)} & 0 \\ \frac{0}{C} & \frac{0}{0.5T \times K_p} \end{bmatrix} \quad (7)$$

The stability of the system can be determined by calculating the Floquet multipliers or the eigenvalues of the fundamental solution matrix  $\mathbf{M}$ . Common problems that have to be addressed here are the location of the limit cycle and the times at which the switchings take place. This can be achieved numerically by deriving a nonlinear function

$g(d_i)$  whose root will define the switching instant [Fossas, and Olivar, 1996] and [Giaouris, Banerjee, Zahawi and Pickert, 2008]. Once the switching instances have been identified, utilizing the fact that the system is linear time invariant (LTI) before and after the switching, it is possible to locate the limit cycle. Once these values are found, the monodromy matrix can be expressed as a function of the input voltage using (3), (6) and (7), and its eigenvalues can be calculated. Fig. 6 shows the eigenvalues of the system for different values of the input voltage clearly indicating the loss of stability through a smooth period doubling bifurcation around 32.3 V as predicted by the results presented in Figs. 2-4. At this point we would like to note that these results could have also been obtained by using the Poincare map but then the analysis would have been more complicated as the overall formula for the Jacobian of the Poincare map would have to include all the switchings [Fang and Abed, 2001].

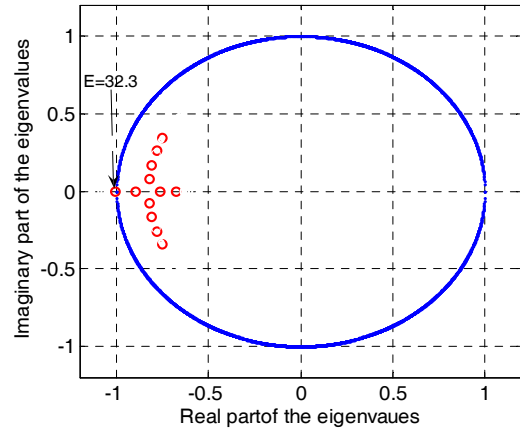


Figure 6. Loci of the eigenvalues of  $\mathbf{M}$

## 5 Control of Bifurcation

In addition to its simplicity, the stability analysis presented in the previous section offers an insight into the behaviour of the system that can be used to evolve control strategies to avoid instabilities. The control requirement here is not only to stabilise the period-1 orbit but also to keep the same steady state value, which implies keeping the location of the orbit almost unchanged. First of all we note that the stability of the system is governed by the eigenvalues of the state transition matrix over a clock cycle (the monodromy matrix), and this matrix is in turn influenced by the state transition matrices across the switching events (the saltation matrices). Hence it is possible to stabilize the orbit without changing its location by manipulating the saltation matrices. Thus we aim at a control action that will change  $\mathbf{M}$  but not  $d_iT$ ,  $\mathbf{x}(d_iT)$ ,  $\mathbf{x}(0)$ .  $\mathbf{S}$  can be influenced by changing the smooth vector fields before and after the switching, and the switching manifold. In practice we cannot change the vector fields as this would imply the physical re-design of the converter. But it is possible to alter the switching manifold(s). To avoid a big change that would change the location of the limit cycle we aim at small changes in  $h$  that will cause “significant” changes in  $\partial h / \partial \mathbf{x}$  and  $\partial h / \partial t$ .

### 5.1 Control Based on the Change of the Upper Limit of the Ramp Signal

The system can be stabilized and the eigenvalues of the monodromy matrix pushed back inside of the unit circle by

modifying the peak value of the ramp signal ( $V_U$ ) to ( $a_1 V_U$ ) with the value of  $a_1$  chosen to determine the desired location. The effect of this change is to alter the time derivative of  $h$  to influence the saltation matrices. Using the theory presented in the last section it is possible to create an analytical expression of the Floquet multipliers as a function of  $a_1$ . Hence, by numerically solving the non-linear transcendental equation  $|eig(\mathbf{M}(T,0))| - 0.824 = 0$ , it is possible to locate the eigenvalues at a predefined location (in this case at a circle of radius 0.824) which indicates stable period-1 behaviour. Corresponding values of  $a_1$  for different values of input voltage can then be calculated (Fig. 7). Experimental waveforms of the output voltage and the inductor current at 34 V are presented in Fig. 8 showing that the system is operating in period-1 operation. Note that according to Fig. 4 the system is unstable at an input voltage of 34V without the proposed control.

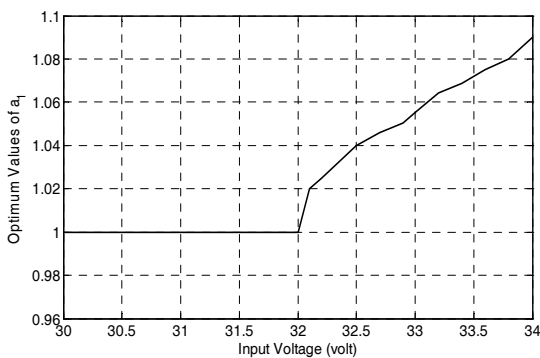


Figure 7. Values of  $a_1$  calculated to place the eigenvalues at a circle of radius 0.824-change of the ramp signal

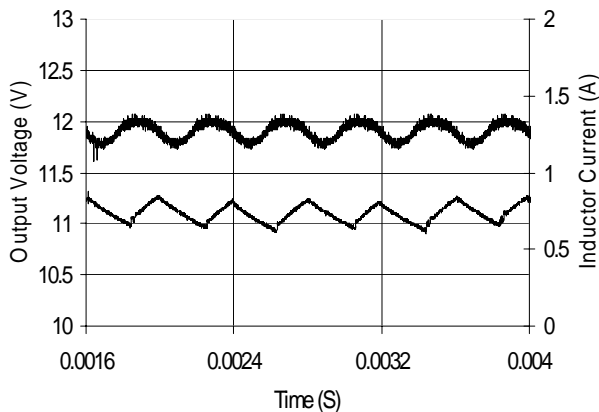


Figure 8. Experimental results with the controller at input voltage of 34 V.

### 5.2 Control Based on an Additional Sinusoidal Signal

Another control method is based on adding a sinusoidal signal to the switching manifold  $h$ , this can be made by changing the value of  $V_{ref}$  to  $V_{ref}(1 + a_2 \sin(\omega t))$ , where  $\omega = 2\pi/T$  and the values of  $a_2$  are chosen to determine the desired location. The effect of this change on the saltation matrix can be seen by deriving the time derivative of  $h_1(X(d_1T))$ :

$$\frac{\partial h_1(X(d_1T))}{\partial t} = -\omega V_{ref} a_2 \cos(\omega t) - \frac{(V_U - V_L)}{0.5T \times K_p} \quad (8)$$

It is obvious from (8) that altering the value of  $a_2$  will have an effect on the time derivative and hence  $\mathbf{S}_1$  and the eigenvalues of the monodromy matrix. Again we can locate

the eigenvalues at any chosen location. The relation between the change of the input voltages and the required values of  $a_2$  for a radius of 0.824 are shown in Fig. 9. The response of the system while the input voltage changes suddenly from 30 to 35V (at 0.1 sec.) is shown in Fig. 10. It is clear that the system, after a very small transient, will settle down quickly to the stable period 1 limit cycle.

This method of stabilising an unstable orbit by another signal at the same frequency is referred to as ‘‘resonant control’’ and it has been empirically applied to a PWM controlled buck converter [Zhou, Tse, Qiu, and Lau, 2003]. But, by using the saltation matrix approach it is possible to carefully design the controller and avoid using trial and error approaches which may lead to instability.

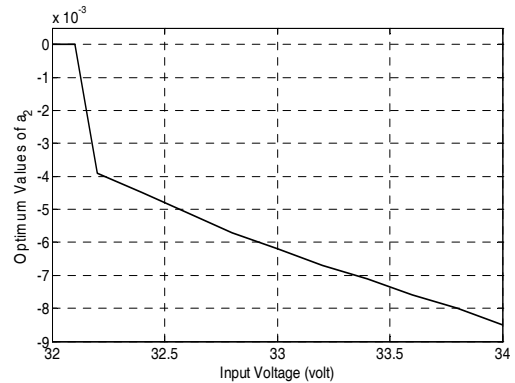


Figure 9. Values of  $a_2$  calculated to place the eigenvalues at a circle of radius 0.824-additional sinusoidal signal.

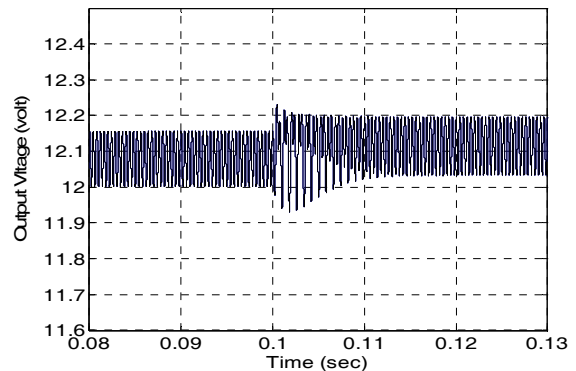


Figure 10. Response of the controller when the input voltage is changed

### 5.3 Control Based on Additional Control Signal Proportional to the Output Voltage

Another control method is based on introducing a change to the normal to the switching manifold. In this method, we slightly change the magnitude of the normal vector  $\mathbf{n}$  so that  $\mathbf{n} = [k_p(1 + a_3) \ 0]^T$ . This will have an influence on the saltation matrices  $\mathbf{S}_1$  and  $\mathbf{S}_2$  thus changing the position of the eigenvalues of the system. The relation between the change of the input voltages and the required values of  $a_3$  are shown in Fig. 11. The response of the system when the input voltage changes from 30 to 35V is shown in Fig. 11. The system settles to the stable period 1 limit cycle after a brief transient.

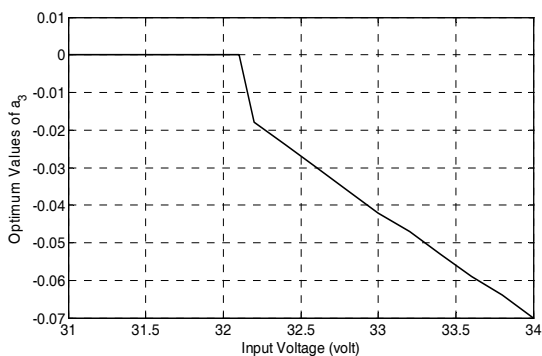


Figure 11. Values of  $a_3$  calculated to place the eigenvalues at a circle of radius 0.824-proportional control signal

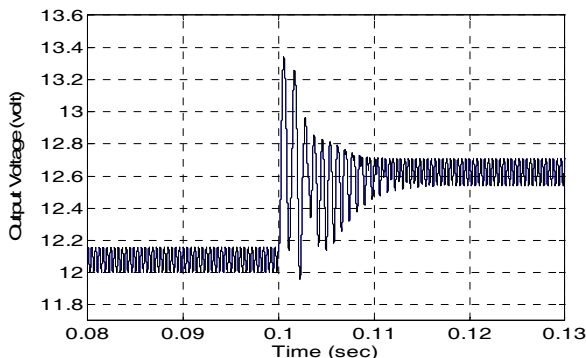


Figure 12. Response of the controller when the input voltage is changed

It is clear that all three controllers extend the range of period one operation. However the third controller which is based on additional control signal proportional to the output voltage has a higher steady-state error.

## 6 Conclusion

In this paper, the stability of the buck converter controlled by double-edged PWM waveform was analysed using the complete-cycle solution matrix. Based on the expression of the saltation matrices, we have proposed and demonstrated three controllers to control the first period doubling to extend the parameter range for stable period-1 operation. The supervising control laws are based on suitably changing the switching manifolds so that the orbit will be stabilised without altering its location, i.e. by keeping the same average value. All controllers were analytically, numerically, and experimentally validated.

## References

- Aizerman, M. A. and Gantmakher, F. R. (1958). On the stability of periodic motions, *Journal of Applied Mathematics and Mechanics (translated from Russian)*, pp. 1065–1078.
- Banerjee, S., Ott, E., Yorke, J. A., Yuan, G-H., (1997). Anomalous bifurcations in dc-dc converters: Borderline collisions in piecewise smooth maps, *IEEE Power Electronics Specialists' Conference*, St. Louis, Missouri, USA, pp.1337-1344.
- Banerjee, S. and Chakrabarty, K. (1998). Nonlinear modeling and bifurcations in the boost converter", *IEEE Transactions on Power Electronics*, vol.13, no.2, pp.252-260.
- Banerjee, S. and Verghese, G. C., (2001). *Nonlinear phenomena in power electronics: Attractors, bifurcations, chaos, and nonlinear control*. New York, USA: IEEE Press.
- Baushev, V. S., Zhusubaliev, Zh. T., Kolokolov, Yu. V., and Terekhin, I. V., (1992). Local stability of periodic solutions in sampled data control systems, *Automation and Remote Control*, vol. 53, no. 2, pp. 865-871.
- Bleich, M. E. and Socolar, J. E. S. (1996). Stability of periodic orbits controlled by time-delayed feedback," *Phys. Lett. A*, vol. 210, pp. 87–94.

- Chakrabarty, K., Poddar, G. and Banerjee, S. (1996). Bifurcation Behaviour of the Buck Converter, *IEEE Transactions on Power Electronics*, vol.11, no.3, pp.439-447.
- Di Bernardo, M., Garofalo, F., Glielmo, L. and Vasca, F., (1998). Switchings, bifurcations and chaos in DC/DC converters, *IEEE Transactions on Circuits and Systems-I*, vol. 45, no. 2, pp. 133–143.
- Di Bernardo, M. and Vasca, F. (2000). On discrete-time maps for the analysis of bifurcations and chaos in DC/DC converters, *IEEE Transactions on Circuits and Systems-I*, vol. 47, no. 2, pp. 130–143.
- Dranga, O., Buti, B., Nagy, I. and Funato, H., (2005). Stability analysis of nonlinear power electronic systems utilizing periodicity and introducing auxiliary state vector, *IEEE Transactions on Circuits and Systems-I*, vol. 52, no. 1 pp. 168–178.
- Fang, C.-C and Abed, E. H., (2001). Sampled-data modelling and analysis of the power stage of PWM DC/DC converters, *International Journal of Electronics*, vol. 88, no. 3, pp. 347 – 369.
- Filippov, A. F., (1988). *Differential equations with discontinuous righthand sides*. Dordrecht: Kluwer Academic Publishers.
- Fossas, E. and Olivar, G. (1996). Study of chaos in the buck converter, *IEEE Transactions on Circuits and Systems-I*, vol. 43, no. 1, pp. 13–25.
- Giaouris, D., Elbkosh, A., Pickert, V., Zahawi, B and Banerjee, S., (2006). Control of period doubling bifurcations in dc-dc converters, in *International Conference Control 2006*, (Glasgow - Scotland)
- Giaouris, D., Elbkosh, A., Banerjee, S., Zahawi, B and Pickert, V., (2006). Control of switching circuits using complete-cycle solution matrices. *IEEE International Conference on industrial Technology (ICIT)*, Mumbai, India.
- Giaouris, D., Banerjee, S., Zahawi, B and Pickert, V., (2008) Stability Analysis of the continuous conduction mode buck converter via filippov's method, *Accepted for publication IEEE Transactions on Circuits and Systems I*
- Hiskens, A. and Pai, M. A., (2000). Trajectory sensitivity analysis of hybrid systems, *IEEE Transactions on Circuits and Systems-I*, vol. 47, no. 2, pp. 204–220.
- Leine, R. I., Campen, D. H. V., and de Vrande, B. L. V. (2000) Bifurcations in nonlinear discontinuous systems, *Nonlinear Dynamics*, vol. 23, pp. 105–164.
- Leine, R. I. and Nijmeijer, H., (2004) *Dynamics and Bifurcations of Non-Smooth Mechanical Systems*. Springer.
- Ott, E., Grebogi, C. and Yorke, J. A., (1990). Controlling chaos, *Phys. Rev. Lett.*, 64, 1196–1199.
- Pyragas, K. (2001) Control of chaos via an unstable delayed feedback controller. *Physical Review Letters*, vol. 86, no.11 :2265–2268.
- Tse, C.K. and Di Bernardo, M. (2002). Complex Behavior in Switching Power Converters," *Proceedings of IEEE*, Special Issue on Applications of Nonlinear Dynamics to Electronic and Information Engineering, vol. 90, no. 5, pp. 768-781.
- Tse, C. K. (2003). *Complex Behavior of Switching Power Converters*. Boca Raton, USA: CRC Press.
- Verghese, G. C., Elbuluk, M. E. and Kassakian, J. G. (1986). A general approach to sampled-data modelling for power electronic circuits, *IEEE Transactions on Power Electronics*, vol. PE-1, no. 2, pp. 76–89.
- Yuan, G-H., Banerjee, S., Ott, E. and Yorke, J.A., (1998). Border-collision bifurcations in the buck converter," *IEEE Transactions on Circuits & Systems -- I*, vol.45, no. 7, pp.707-716.
- Zhou, Y., Tse, C. K. Qiu, S. S., and Lau, F. C. M. (2003). Applying resonant parametric perturbation to control chaos in the buck dc/dc converter with phase shift and frequency mismatch considerations," *International Journal of Bifurcation and Chaos*, vol. 13, no. 11, pp. 3459–3471.
- Zhusubaliyev, Zh. T., Soukhoterlin, E. A., and Mosekilde, E., (2001). Border-collision bifurcations and chaotic oscillations in a piecewise-smooth dynamical system, *International Journal of Bifurcation and Chaos*, vol. 11, no. 12, pp. 2977-3001.